CHAPTER IV

RESULTS AND DISCUSSION

Since the physical properties of all PAMEs studied (such as boiling point and vapor pressure) were quite different, retention factors and enantioselectivities of each analyte at particular temperature could not be directly compared. As a consequence, retention factors and enantioselectivities obtained over a temperature range will be considered to provide better information about the analyte-stationary phase interactions.

All plots of ln k' versus 1/T of each enantiomer gave linear relationship with good correlation coefficient (R^2 greater than 0.9989). Slope and y-intercept obtained from ln k' versus 1/T plots of all analytes were used to calculate enthalpy change (ΔH) and entropy change (ΔS), respectively. When the enantiomers could be separated, enthalpy difference ($\Delta \Delta H$) and entropy difference ($\Delta \Delta S$) could be achieved from the difference in ΔH and ΔS of each pair of enantiomers.

4.1 Enthalpy change ($-\Delta H$) and entropy change ($-\Delta S$)

The enthalpy change ($-\Delta H$) represented the strength of interaction between an analyte and a stationary phase. More negative value (larger value) showed the stronger interaction. While the entropy change ($-\Delta S$) represented the loss of degree of freedom associated with the interaction between an analyte and a stationary phase.

The enthalpy change and the entropy change obtained from both columns were presented in Figures 4.1-4.4. On ASiAc column, no PAMEs could be separated into their enantiomers. All PAMEs had enthalpy change values ($-\Delta H$) in the range from 12.5-15.9 kcal/mol, with the average value of 13.65±0.81 kcal/mol (Figure 4.1). This result suggested that the major influence toward the interaction between analyte and this stationary phase would come from phenyl and ester groups of

PAMEs. The substituent of analytes showed some influences as $-\Delta H$ values of nitro- and cyano-containing PAMEs were slightly higher than others. For halide-containing PAMEs, $-\Delta H$ values were in the order of Br > Cl > F. Increasing number of substitution did not give significantly higher $-\Delta H$ values. For mono-substituted PAMEs, the effect of the substituent position was also observed as all the *para*-substituted PAMEs had slightly higher $-\Delta H$ values than *ortho-* and *meta*-isomers. Similar trend was also observed for $-\Delta S$ values, but the values were very similar with the average of 18.03±0.54 cal/mol·K (Figure 4.2).

On GSiAc column, 34 PAMEs could be separated into their enantiomers. All more retained enantiomers had $-\Delta H_2$ values in the range from 13.3-20.5 kcal/mol, with the average value of 15.73±1.43 kcal/mol (Figure 4.3). Previous study on BSiAc by Rodthongkum [12] reported the average $-\Delta H_2$ values of 14.54±1.06 kcal/mol. Comparing the effect of cyclodextrin ring size, it was found that the average $-\Delta H_2$ values between analytes and stationary phases increased with the increasing ring size from ASiAc < BSiAc < GSiAc column. Nitro- and cyano-containing PAMEs still showed slightly higher $-\Delta H$ values than other analytes on GSiAc column. However, there was no apparent trend for other types of substituent or substituent position. Likewise, there was no apparent trend for $-\Delta S_2$ values (Figure 4.4).
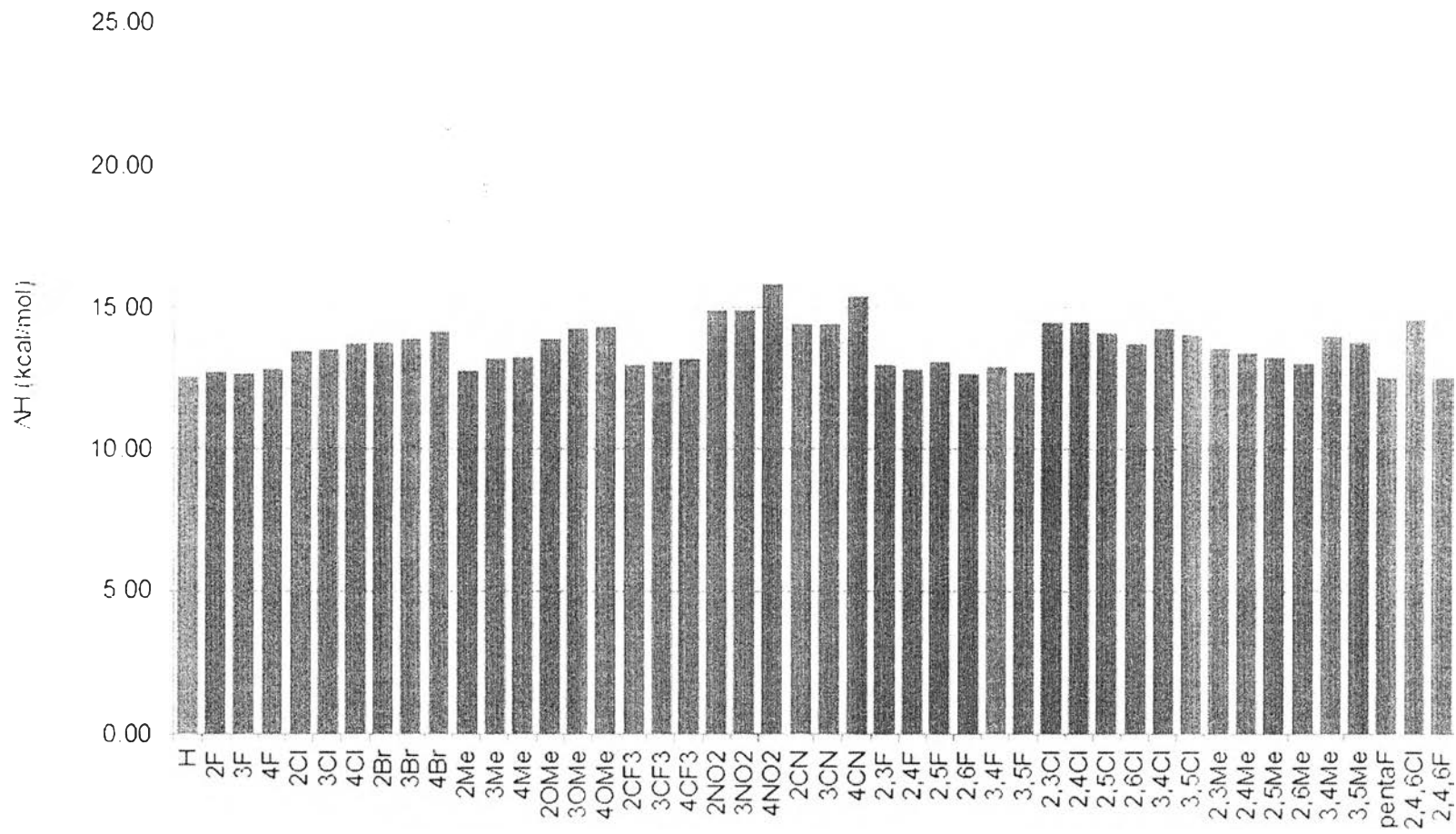
Figure 4.1 Enthalpy change of enantiomer (−ΔH, kcal/mol) of PAMEs on ASiAc column, average = 13.65, SD = 0.81

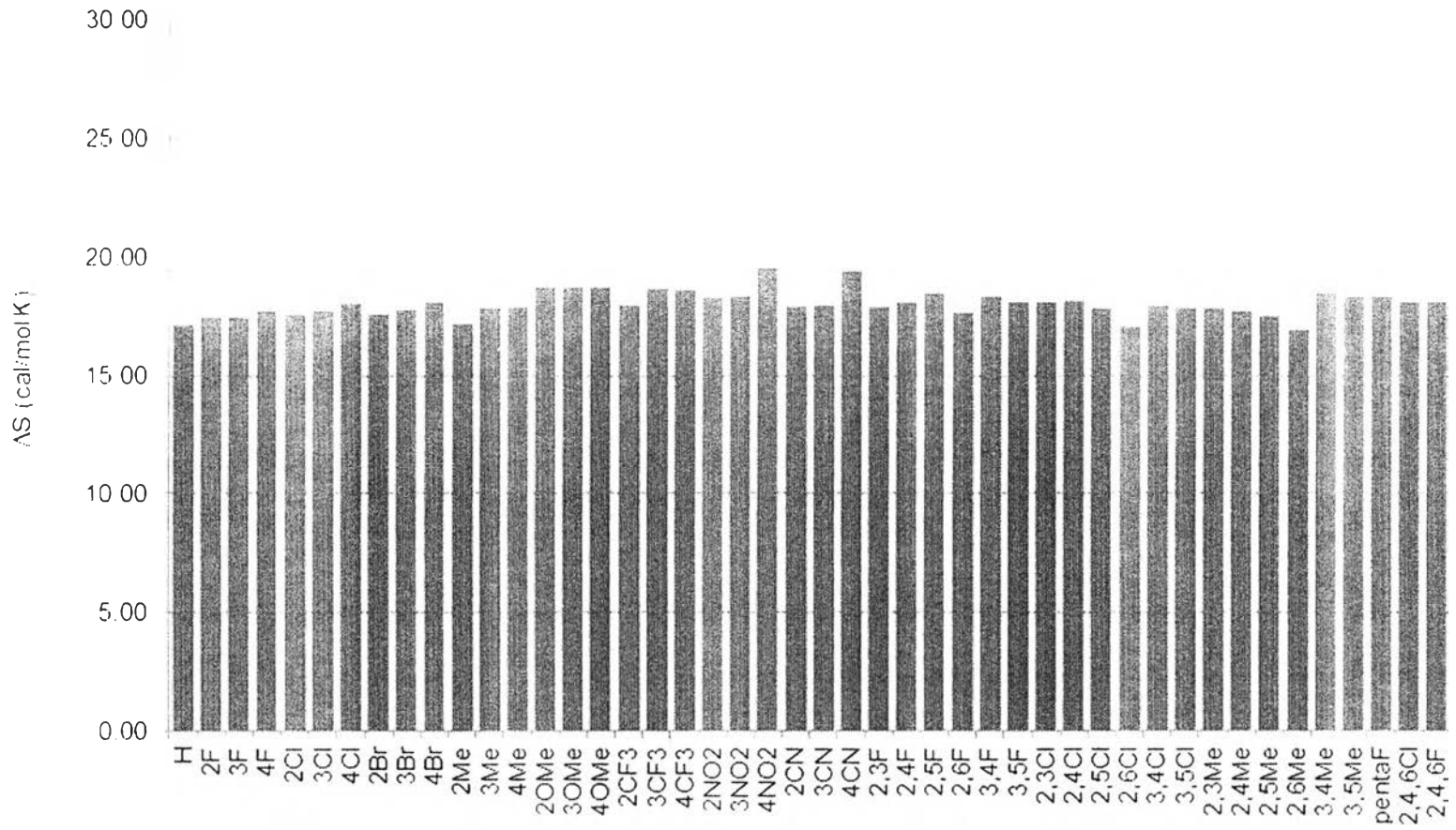Figure 4.2 Entropy change of enantiomer (−ΔS, cal/mol·K) of PAMEs on ASiAc column, average = 18.03, SD = 0.54
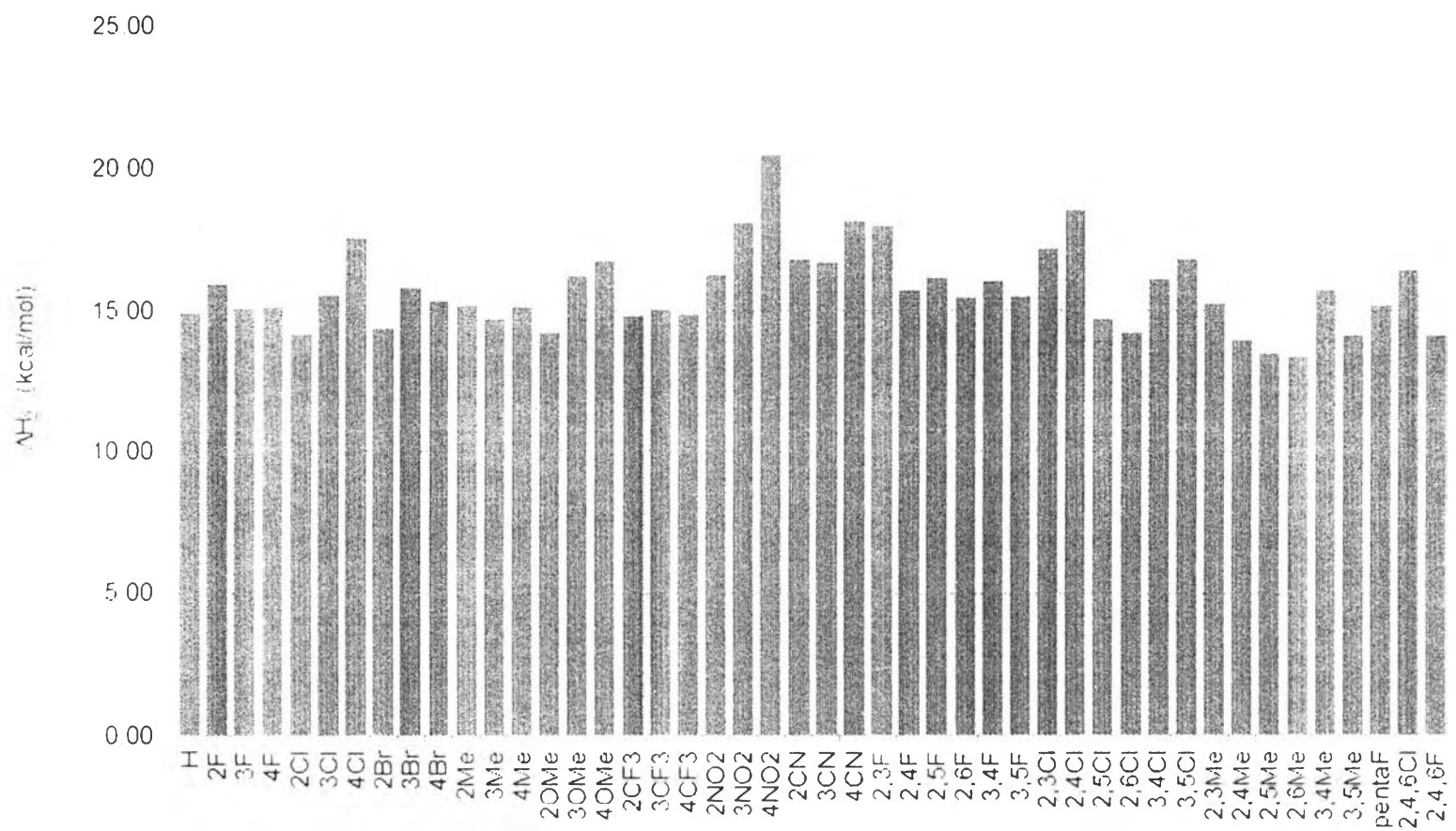
Figure 4.3 Enthalpy change of more retained enantiomer ($-\Delta H_2$, kcal/mol) of PAMEs on GSiAc column, average = 15.73, SD = 1.43
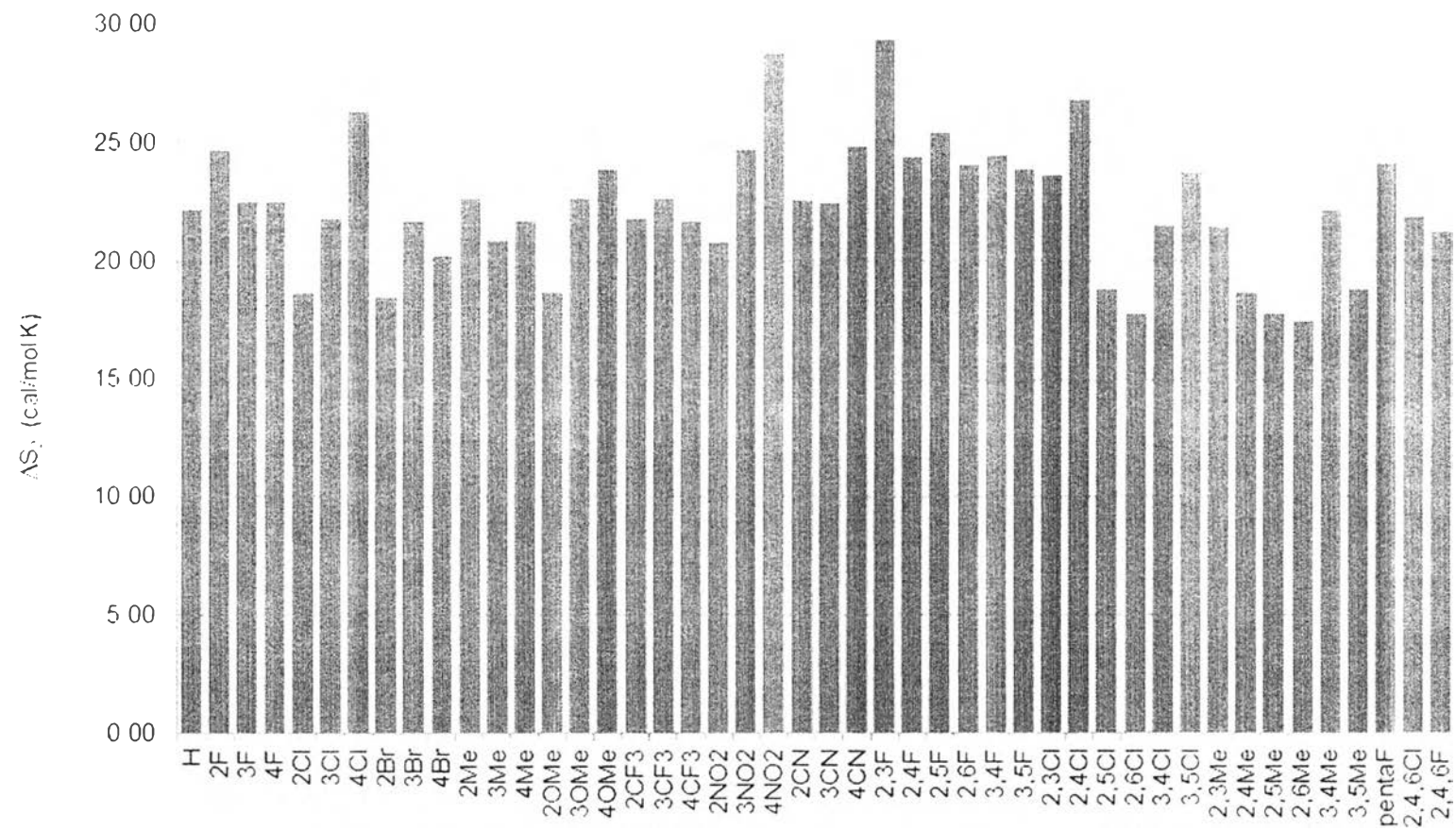
Figure 4.4 Entropy change of more retained enantiomer ($-\Delta S_2$, cal/mol·K) of PAMEs on GSiAc column, average = 22.35, SD = 2.74

4.2 Enthalpy difference ($-\Delta\Delta H$) and entropy difference ($-\Delta\Delta S$)

The enthalpy difference ($-\Delta\Delta H$) represented the chiral discrimination energies between analyte and stationary phase. While the entropy difference ($-\Delta\Delta S$) represented the variation of two entropy values between a pair of enantiomers during chiral recognition process. In this work, $-\Delta\Delta H$ and $-\Delta\Delta S$ were calculated from the difference in ΔH and ΔS of enantiomeric pair using plot of ln k' versus 1/T.

No PAMEs in this study could be separated into their enantiomers by smaller-size derivatized CD, ASiMe column. From forty-six PAMEs, thirty-four analytes could be enantioseparated by GSiMe column. The results indicated the effect of cyclodextrin ring size towards enantioselectivity. The enthalpy difference ($-\Delta\Delta H$) and the entropy difference ($-\Delta\Delta S$) from GSiAc column of all PAMEs studied in this research were presented in Figures 4.5-4.6. Since the trends of $-\Delta\Delta H$ and $-\Delta\Delta S$ obtained from GSiAc column were similar, only $-\Delta\Delta H$ value will be discussed.

In this research, methyl 2-phenoxypropanoate (H) with no substitution on the aromatic ring was used as a reference analyte. H could be enantioseparated by GSiAc column. PAMEs with substitution(s) showed lower $-\Delta\Delta H$ values than H. However, type, position and number of substituent on the aromatic ring of PAMEs influenced the enantiomeric separation at various degrees. Therefore, discussion dealing with enantioseparation was described in three groups according to the numbers of substituent on the aromatic rings which were one, two and more substituent(s) correspondingly.
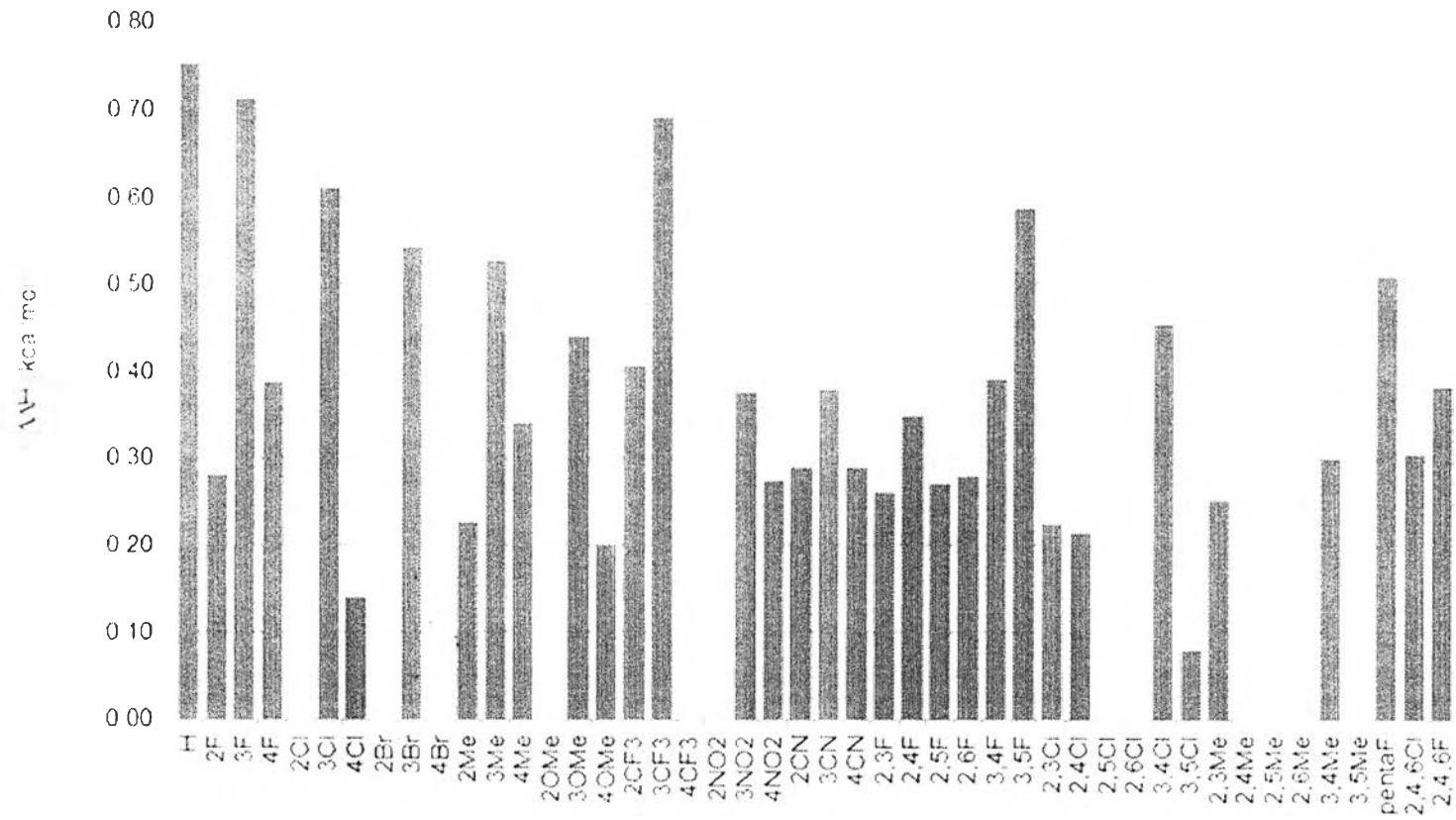
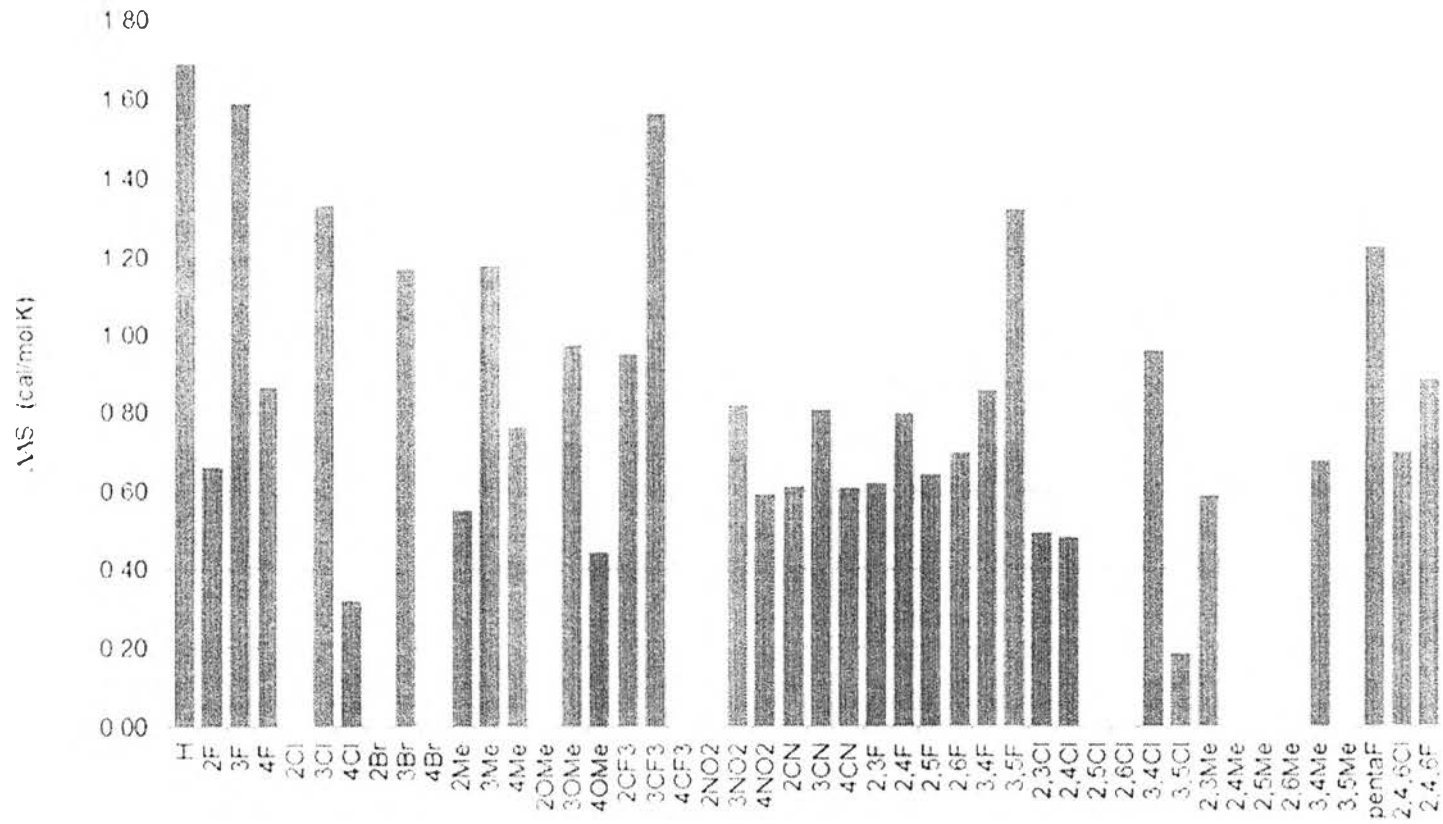**Figure 4.5** Enthalpy difference (−ΔΔH, kcal/mol) of PAMEs on GSiAc column
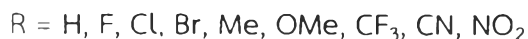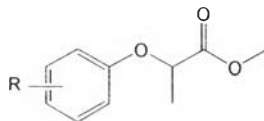
Figure 4.6 Entropy difference (−ΔΔS, cal/mol·K) of PAMEs on GSiAc column

Group 1: PAMEs with mono-substitution on the aromatic ring

R = H, F, Cl, Br, Me, OMe, CF_3, CN, NO_2

Enantiomers of PAMEs in Group 1 were methyl 2-phenoxypropanoate derivatives with mono-substitution on the aromatic ring as shown above. Types of substituent were fluoro, chloro, bromo, methyl, methoxy, trifluoromethyl, cyano and nitro.

GSiAc column could separate eighteen enantiomers from twenty-four enantiomers of mono-substituted PAMEs as seen from enthalpy difference ($-\Delta\Delta H$) in Figure 4.7. Six mono-substituted PAMEs could not be enantioseparated over the temperature range studied.

For twenty four isomers of mono-substituted PAMEs, $4NO_2$ showed the largest $-\Delta H$ value (Figure 4.3). The result corresponded to largest slope value from the plot of ln k' versus 1/T indicating the largest increase in k' value with a decrease in temperature; thus leading to longer analysis time. However, strong retention factor did not necessarily correlate to high enantioselectivity.

For methyl 2-phenoxypropanoate (H), a reference analyte, it could be separated with this stationary phase with the largest $-\Delta\Delta H$ value. PAMEs with substitution on the aromatic ring showed lower $-\Delta\Delta H$ values than H. The influence of type and position of substituent on the aromatic ring of mono-substituted PAMEs on enantioseparation was studied.
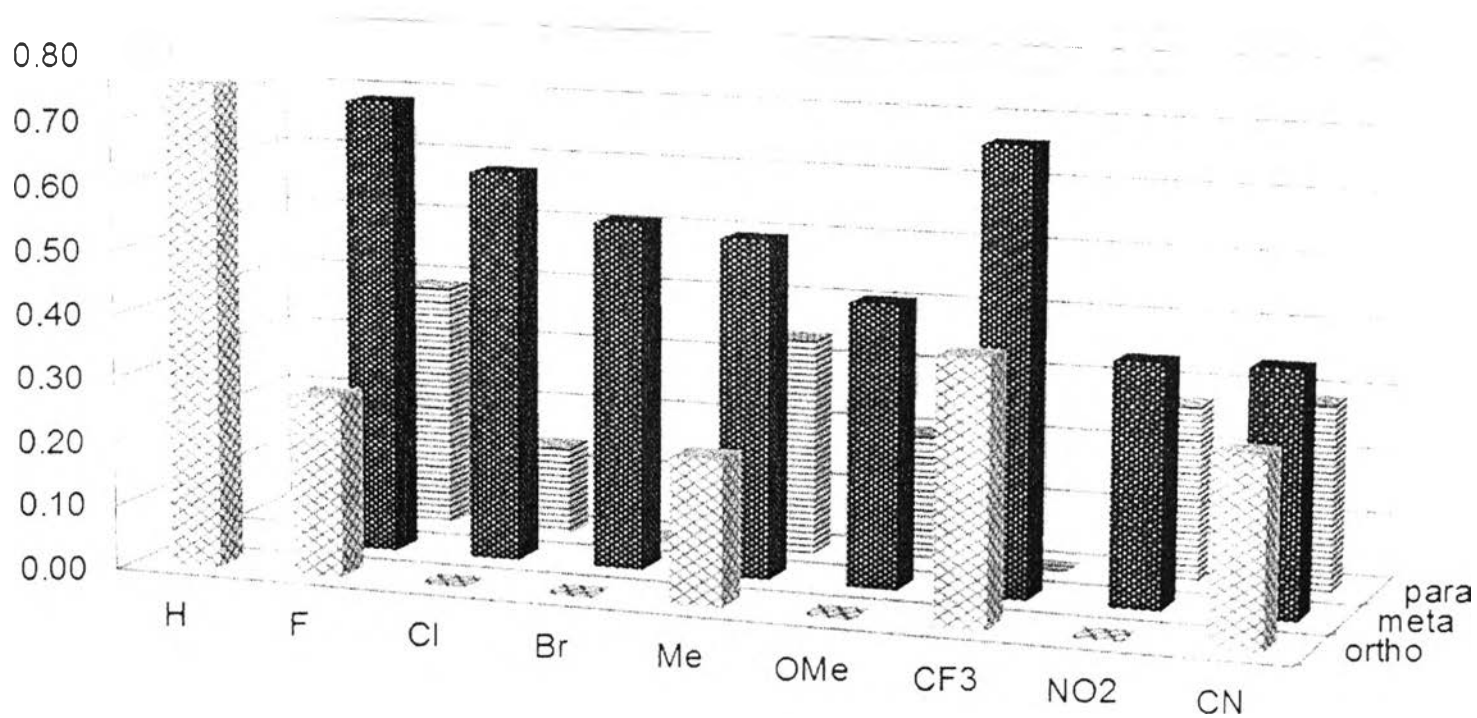
−ΔΔH (kcal/mol)

Figure 4.7 Enthalpy difference (−ΔΔH, kcal/mol) of mono-substituted PAMEs on GSiAc column

From Figure 4.7, it was quite clear that the position of substituent on the aromatic ring of mono-substituted PAMEs was strongly influenced on enantioseparation (as shown by $-\Delta\Delta H$ values). It was found that all eight *meta*-substituted PAMEs could be enantioseparated. In addition, *meta*-substituted PAMEs showed higher $-\Delta\Delta H$ values than *ortho*- or *para*-substituted isomers for all types of substitution. Considering *ortho*- and *para*-substituted PAMEs, six *para*-substituted isomers were enantioseparated and only four *ortho*-substituted isomers were enantioseparated. In most cases, *para*-substituted isomers showed higher $-\Delta\Delta H$ values than *ortho*-substituted isomers, except for trifluoromethyl-substituted PAMEs where **4CF$_3$** could not be enantioseparated.

The influence of the position of substituent towards retention and enantioselectivity was shown as an example. Relationship between ln k'$_2$ versus 1/T and between ln α versus 1/T of H and three monofluoro-substituted PAMEs on GSiAc column were shown in Figures 4.8-4.9. All analytes had similar retention factors with slightly higher k' value for **4F** at every temperature studied (Figure 4.8), indicating longer analysis time for **4F**. As the temperature decreased, all analytes similarly more retained as indicated by very similar slope between ln k'$_2$ versus 1/T plots. Nevertheless, their enantioselectivities were different. H and **3F** had higher enantioselectivities than **2F** and **4F** at every temperature studied (Figure 4.9). As the temperature decreased, enantioselectivities increased for all analytes. H and **3F** showed sharper slopes and higher $-\Delta\Delta H$ values than **2F** and **4F**, indicating that enantioseparation of H and **3F** could be easily improved with a slight decrease in temperature. Chromatograms demonstrating the effects of temperature and position of substituent on k' and α of H, **2F**, **3F** and **4F** were compared in Figure 4.10. Although **4F** was more retained on this stationary phase, H and **3F** showed better enantioseparation in shorter analysis time. The decrease in temperature by 10 °C improved the separation for H and **3F** better than for **2F** and **4F**. These results suggested that substitution at *meta*-position of the aromatic ring provided good enantioseparation, while substitution at *ortho*-position of the aromatic ring led to poor enantioseparation.
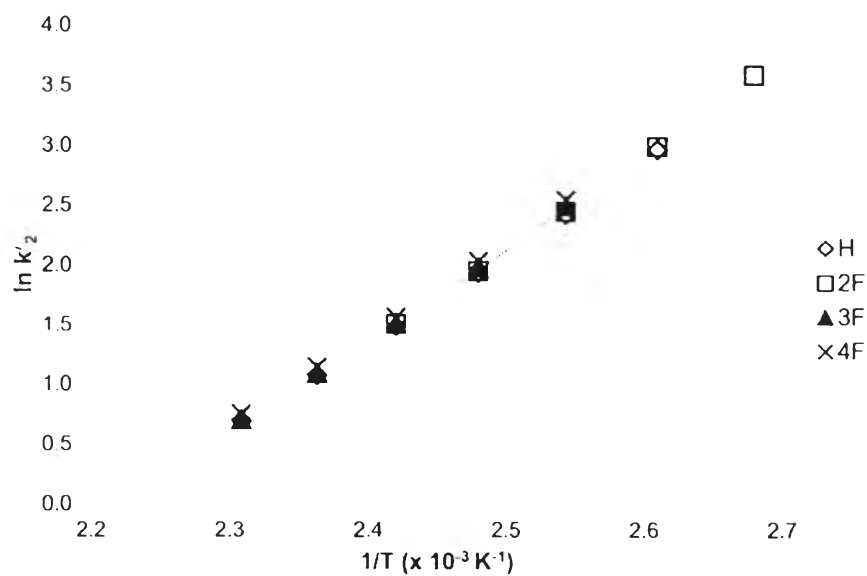
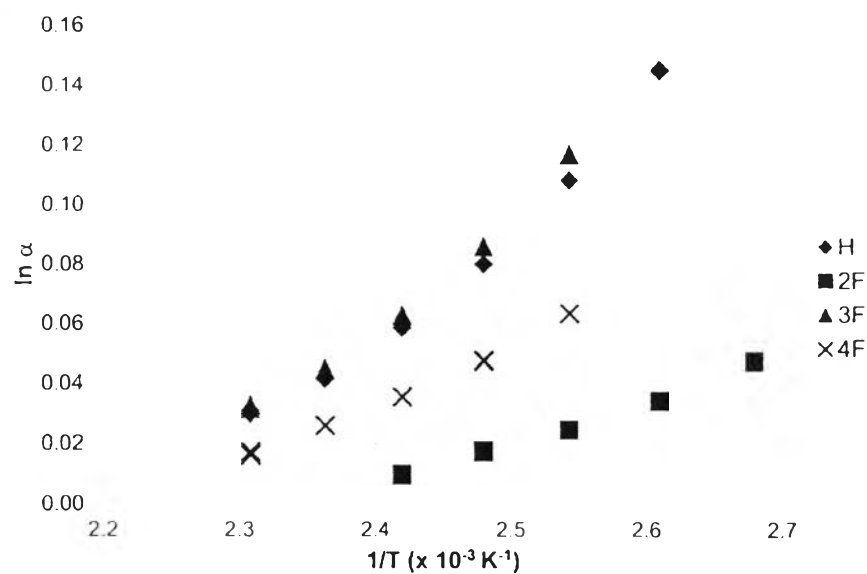**Figure 4.8** Plots of ln k'$_2$ versus 1/T of **H**, **2F**, **3F** and **4F** on GSiAc column

Figure 4.9 Plots of ln α versus 1/T of **H**, **2F**, **3F** and **4F** on GSiAc column

140 °C

$(1/T = 2.42 \times 10^{-3} \, K^{-1})$

130 °C

$(1/T = 2.48 \times 10^{-3} \, K^{-1})$

(a) H $\alpha = 1.060$ $\alpha = 1.083$

(b) 2F $\alpha = 1.010$ $\alpha = 1.017$

(c) 3F $\alpha = 1.064$ $\alpha = 1.089$

(d) 4F $\alpha = 1.036$ $\alpha = 1.049$

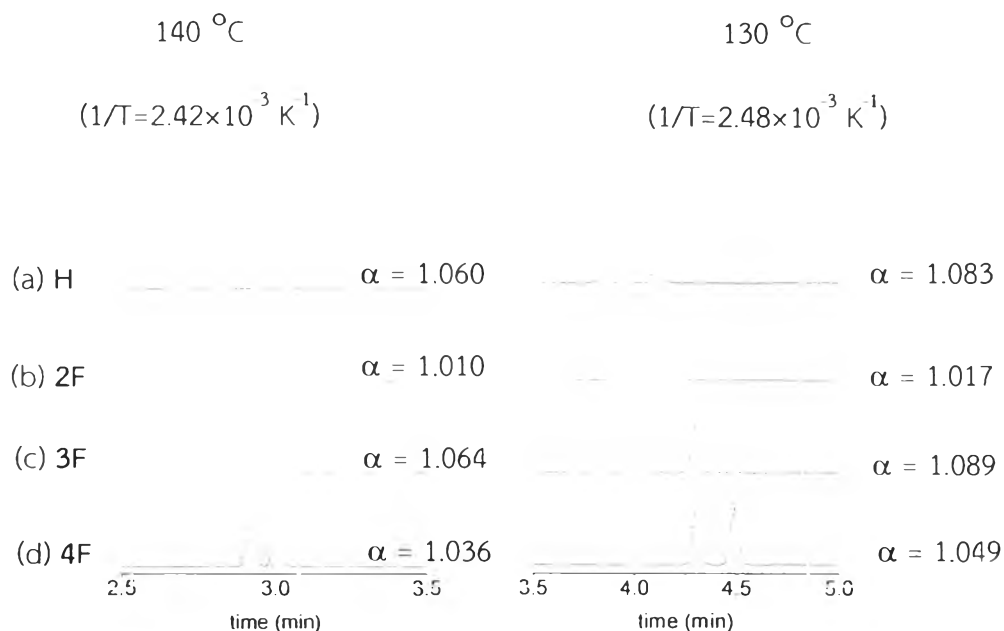| 2.5 | 3.0 | 3.5 | 3.5 | 4.0 | 4.5 | 5.0 |

time (min)   time (min)

Figure 4.10 Chromatograms of (a) H, (b) 2F (c) 3F and (d) 4F at 140 °C (left) and 130 °C (left) on GSiAc column

Next, the influence of type of substituent on the aromatic ring of mono-substituted PAMEs on enantioseparation was studied. Among all *meta*-substituted PAMEs using GSiAc column, $-\Delta\Delta H$ values declined in order of 3F ≈ 3CF$_3$ > 3Cl > 3Br ≈ 3Me > 3OMe > 3CN ≈ 3NO$_2$. Good enantioseparation (higher $-\Delta\Delta H$ values) was observed when the aromatic proton was replaced by high electronegativity substitution such as fluoro and trifluoromethyl. Considering analytes with halogenated substitution, $-\Delta\Delta H$ value decrease in order of 3F > 3Cl > 3Br according to the decreasing electronegativity of substituent (EN_F = 4.0, EN_{Cl} = 2.8, EN_{Br} = 2.7 [34]) and to the increasing size of substituent (r_F = 131 pm, r_{Cl} = 181 pm, r_{Br} = 196 [35]). The effect of type of substituent on *ortho-* and *para*-substituted PAMEs was different from their *meta*-isomers. For *ortho*-substituted PAMEs, **2CF$_3$** showed highest $-\Delta\Delta H$ values. While **4F** showed highest $-\Delta\Delta H$ values among *para*-substituted PAMEs, **4CF$_3$** could not be enantioseparated.

Considering analytes with halogenated substitution at *meta*-position, they were **3F**, **3Cl** and **3Br**. Relationships between ln k′$_2$ versus 1/T and between ln α versus 1/T of **3F**, **3Cl** and **3Br** on GSiAc column were shown in Figures 4.11-4.12. Retention factors at the same temperature were in the order of **3F** < **3Cl** < **3Br**.

Enantioselectivities also showed the same trend but the values were very similar. From k' and α values mentioned above as well as highest $-\Delta\Delta H$ values of **3F**, complete enantioseparation of **3F** could be obtained in shortest analysis time (about 2 minutes at 150 °C). The separation of **3F**, **3Cl** and **3Br** at 160 °C and 150 °C were compared in Figure 4.13.
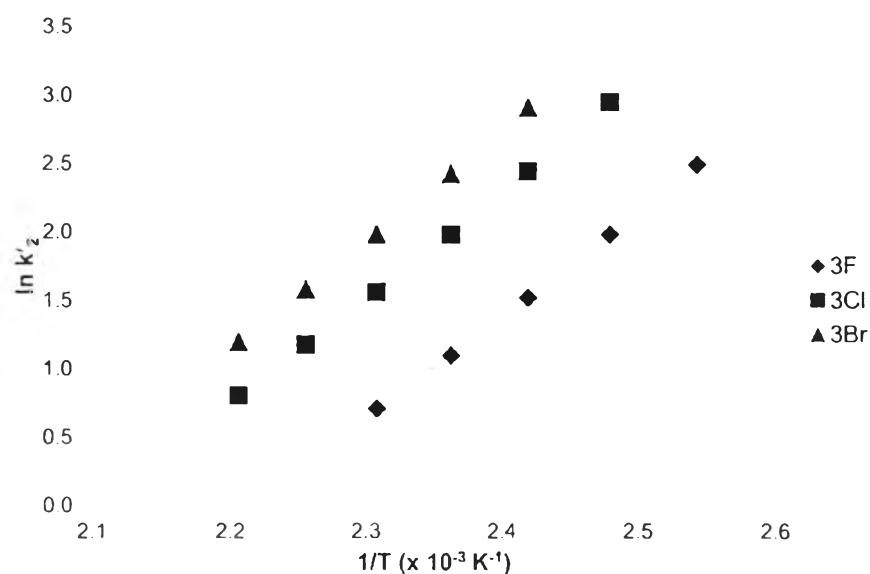

Figure 4.11 Plots of ln k'$_2$ versus 1/T of **3F**, **3Cl** and **3Br** on GSiAc column
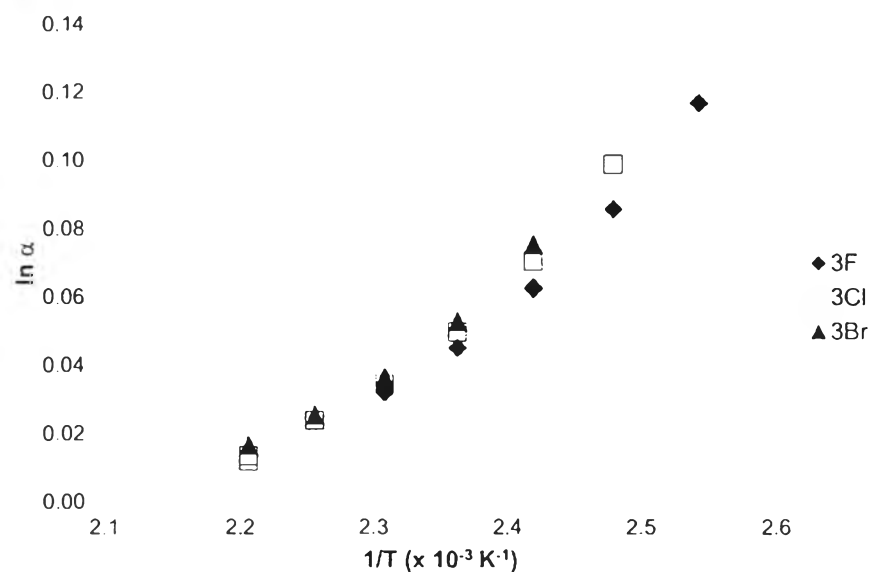

Figure 4.12 Plots of ln α versus 1/T of **3F**, **3Cl** and **3Br** on GSiAc column

160 °C

$(1/T = 2.31 \times 10^{-3} \text{ K}^{-1})$

150 °C

$(1/T = 2.36 \times 10^{-3} \text{ K}^{-1})$

(a) 3F $\quad\quad\quad\quad\quad\quad \alpha = 1.033 \quad\quad\quad\quad\quad\quad\quad\quad\quad \alpha = 1.046$

(b) 3Cl $\quad\quad\quad\quad\quad\quad \alpha = 1.035 \quad\quad\quad\quad\quad\quad\quad\quad\quad \alpha = 1.051$

(c) 3Br $\quad\quad\quad \alpha = 1.037 \quad\quad\quad\quad\quad\quad\quad\quad\quad\quad\quad \alpha = 1.054$

| 1 | 2 | 3 | 4 | 5 | 1 | 2 | 3 | 4 | 5 | 6 | 7 |

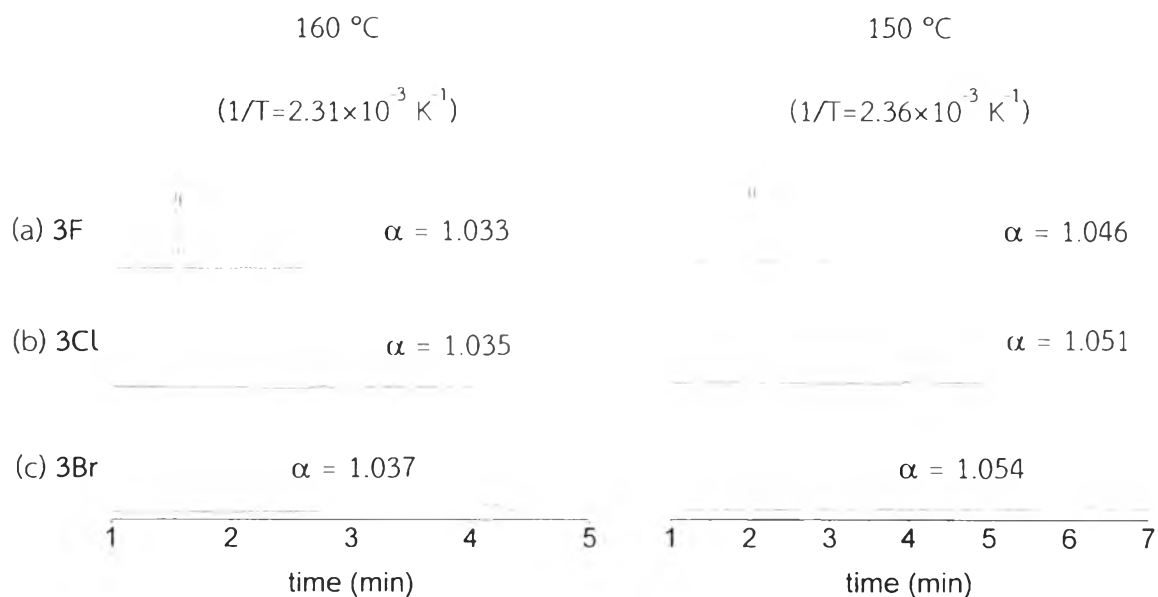time (min) $\quad\quad\quad\quad\quad\quad\quad\quad\quad$ time (min)

Figure 4.13 Chromatograms of (a) **3F**, (b) **3Cl** and (c) **3Br** at 160 °C (left) and 150 °C (right) on GSiAc column

Results from **3Me**, **3OMe** and **3CF₃** were also compared. Relationships between ln k'_2 versus 1/T and between ln α versus 1/T of **3Me**, **3OMe** and **3CF₃** on GSiAc column were shown in Figures 4.14-4.15. **3OMe** had highest retention at every temperature studied. While enantioselectivity of three analytes were very similar at high temperatures, **3CF₃** had the highest enantioselectivity at lower temperature. This is due to higher slope from ln α versus 1/T plot of **3CF₃**, resulting in highest $-\Delta\Delta H$ value. Thus, enantioseparation of **3CF₃** could be easily improved with a slight decrease in temperature. The separation of **3Me**, **3OMe** and **3CF₃** at 150 °C and 140 °C were compared in Figure 4.16.
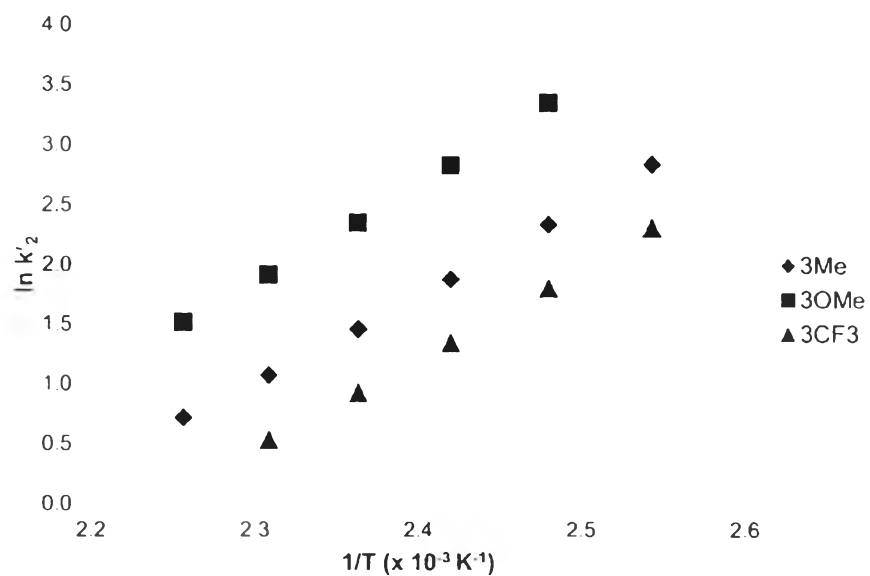
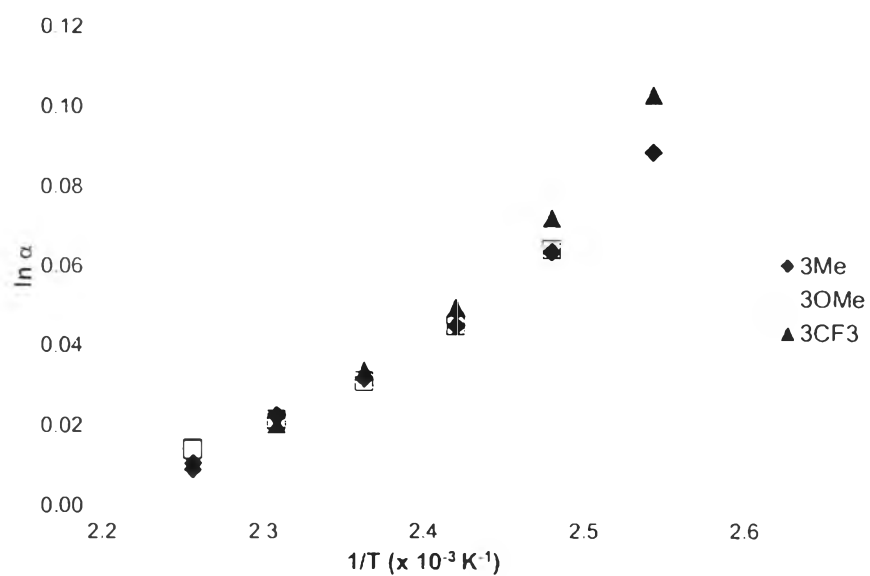Figure 4.14 Plots of ln k′$_2$ versus 1/T of **3Me**, **3OMe** and **3CF$_3$** on GSiAc column

Figure 4.15 Plots of ln α versus 1/T of **3Me**, **3OMe** and **3CF$_3$** on GSiAc column

150 °C

$(1/T=2.36\times10^{-3}\ K^{-1})$

140 °C

$(1/T=2.42\times10^{-3}\ K^{-1})$

(a) 3Me $\alpha = 1.032$ $\alpha = 1.046$

(b) 3OMe $\alpha = 1.032$ $\alpha = 1.046$

(c) 3CF$_3$ $\alpha = 1.034$ $\alpha = 1.051$

time (min)   time (min)
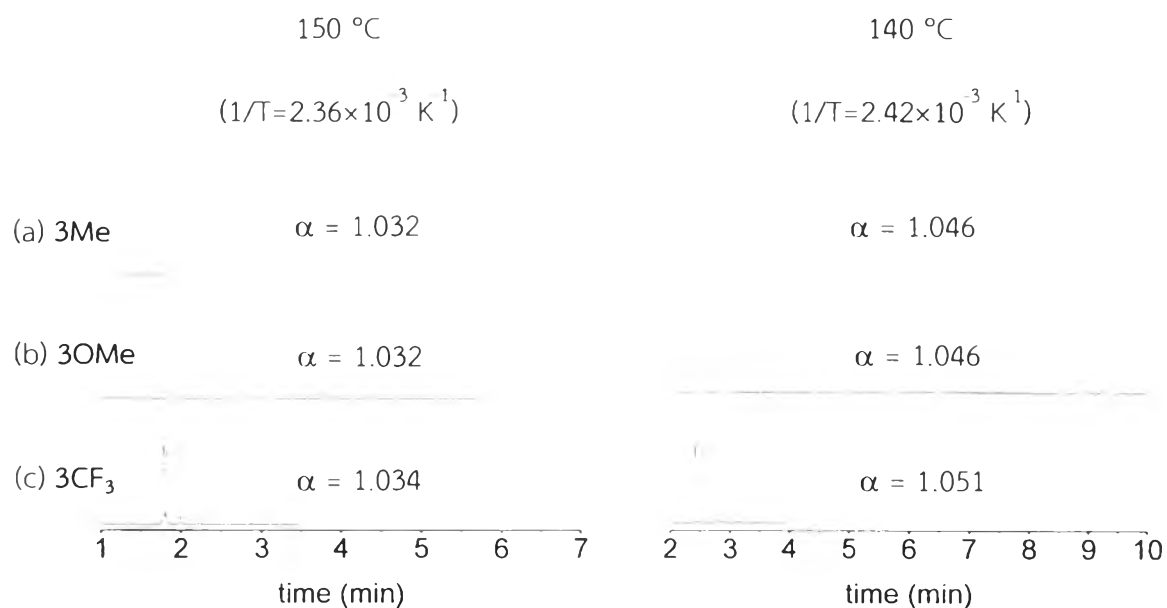
Figure 4.16 Chromatograms of (a) 3Me, (b) 3OMe and (c) 3CF$_3$ at 150 °C (left) and 140 °C (right) on GSiAc column

Results for group 1 PAMEs obtained from GSiAc column were compared to those previously obtained from BSiAc column [12]. BSiAc columns could separate enantiomers of all *meta-* and *para*-substituted PAMEs, with higher $-\Delta\Delta H$ values for most *para*-isomers than *meta*-isomers. However, both BSiAc and GSiAc columns poorly separated enantiomers of *ortho*-substituted PAMEs. Only three and four *ortho*-substituted PAMEs could be enantioseparated by BSiAc and GSiAc columns, respectively. Both columns could not separate enantiomers of 2Br, 2OMe and 2NO$_2$.

Group 2: PAMEs with di-substitution on the aromatic ring

R = F, Cl, Me
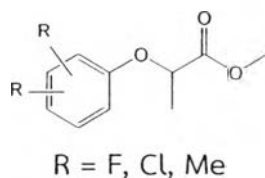
Enantiomers of PAMEs in Group 2 were methyl 2-phenoxypropanoate derivatives with di-substitution on the aromatic ring as shown above. Types of substituent were fluoro, chloro and methyl. GSiAc column could separate twelve enantiomers from eighteen enantiomers of di-substitution PAMEs as seen from enthalpy difference ($-\Delta\Delta H$) in Figure 4.17. Six di-substituted PAMEs could not be enantioseparated over the temperature range studied.

From Figure 4.17, it was quite clear that the type of substituent on the aromatic ring of di-substituted PAMEs was the main influence on enantioseparation (as shown by $-\Delta\Delta H$ values). Among three types of di-substituted PAMEs, all six isomers of difluro-substituted PAMEs could be enantioseparated. Four isomers of dichloro- and only two isomers of dimethyl-substituted PAMEs could be enantioseparated. The highest $-\Delta\Delta H$ value was observed for **3,5F**. The result was similar to that of mono-substituted PAMEs in group 1 where **3F** had the highest $-\Delta\Delta H$ value.
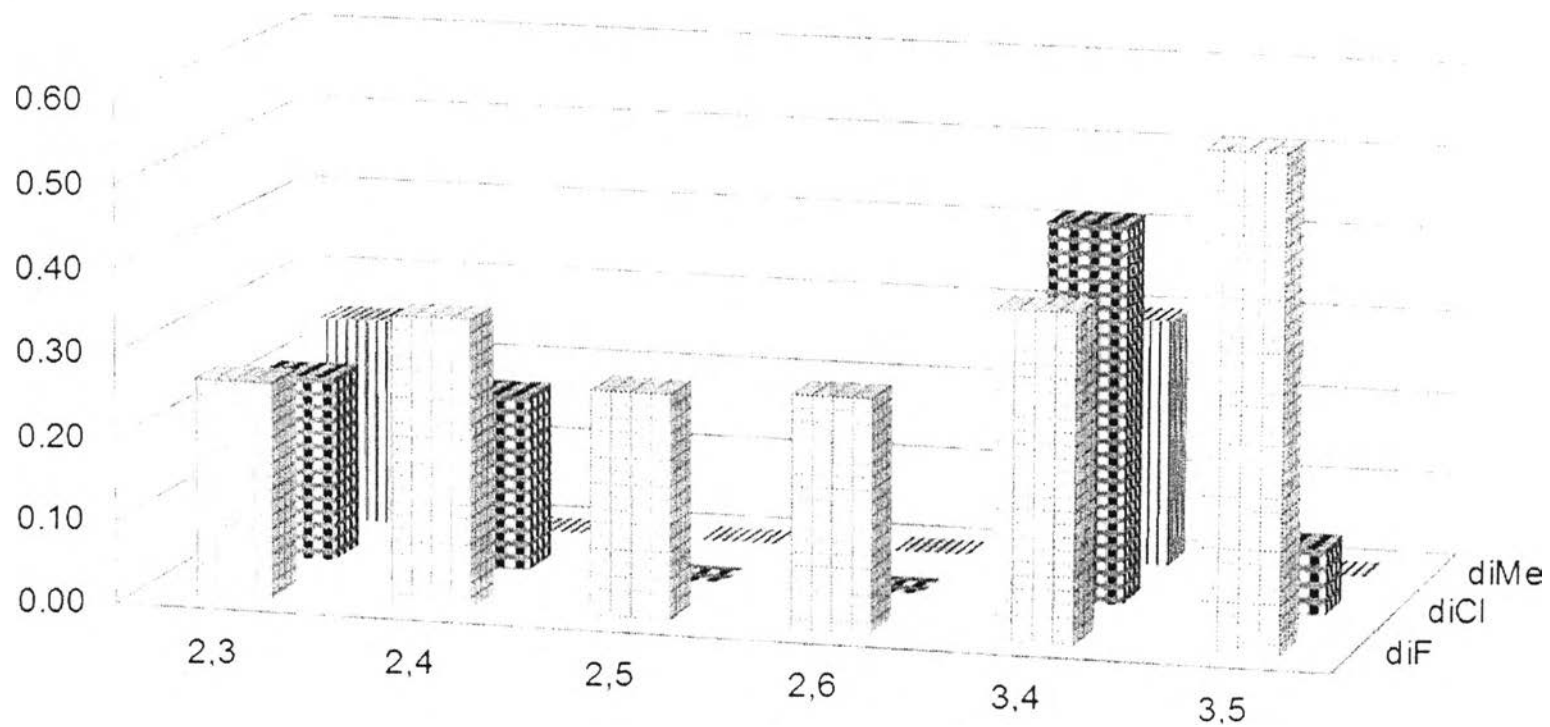
Figure 4.17 Enthalpy difference ($-\Delta\Delta H$, kcal/mol) of di-substituted PAMEs on GSiAc column

Next, the influence of position of substituent on the aromatic ring of di-substituted PAMEs on enantioseparation was studied. It was found that most analytes that could be enantioseparated contained substituent(s) at *meta*-position(s), at either 3- or 5-position or at both positions. These observations also agreed with those obtained from group 1 PAMEs where *meta*-substituted PAMEs showed higher $-\Delta\Delta H$ values than *ortho*- or *para*-isomers. Among all eighteen analytes of di-substituted PAMEs, **3,5F** with two *meta*-substitutions showed the highest $-\Delta\Delta H$ value. However, **3,5Cl** had the lowest $-\Delta\Delta H$ value among four enantioseparated dichloro-substituted isomers and **3,5Me** could not be enantioseparated. Interestingly, all 2,3- and 3,4-disubstituted of PAMEs could be enantioseparated on GSiAc column. This suggested that both type and position of substitution are important factors in enantioseparation.

Relationships between ln k' versus 1/T and between ln α versus 1/T of six dichloro-substituted PAMEs on GSiAc column were shown in Figures 4.18-4.19. At the same temperature, retention of all six isomers varied slightly in the order of **2,4Cl** > **2,3Cl** > **3,4Cl** > **3,5Cl** > **2,5Cl** > **2,6Cl** (Figures 4.18 and 4.20). However, their enantioselectivities were different. **3,4Cl** had the best enantioselectivity at all tested temperatures and also had higher slope and higher $-\Delta\Delta H$ value than other isomers. Thus, enantioseparation of **3,4Cl** could be the most easily improved with a slight decrease in temperature. Chromatograms of six dichloro-substituted PAMEs at 150 °C were shown in Figure 4.20. At 150 °C, **3,4Cl** showed complete resolution while **3,5Cl** could not be enantioseparated. In addition, temperature had very small effect towards enantioselectivity of **3,5Cl** as the α slightly increased with the decrease in temperature. The temperature must be lower to observe enantioseparation of **3,5Cl**, thus leading to long analysis time.
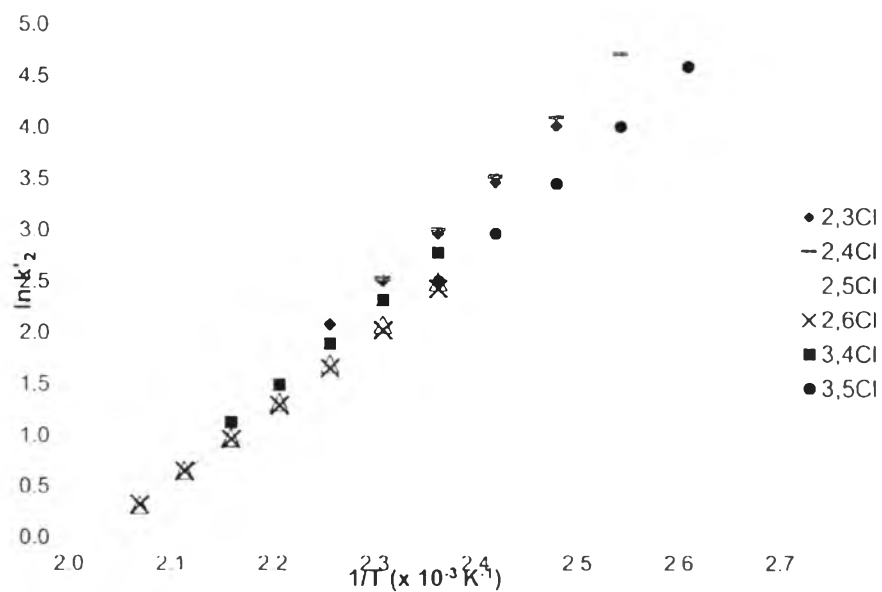
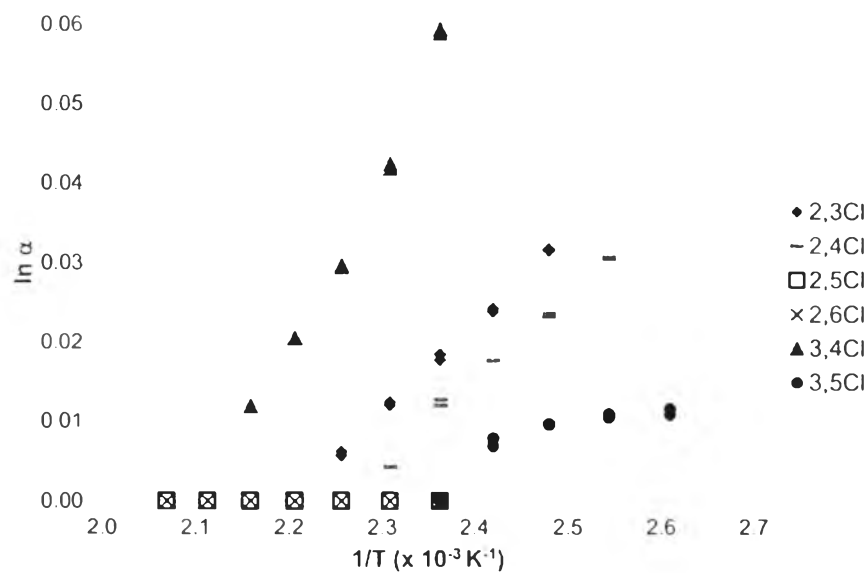**Figure 4.18** Plots of ln k' versus 1/T of six dichloro-substituted PAMEs on GSiAc column

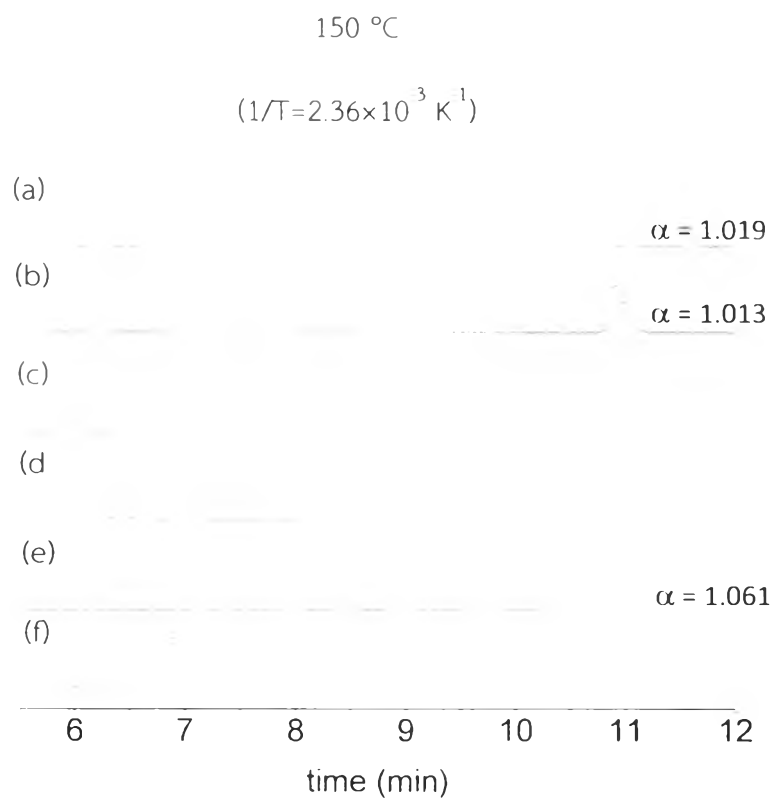**Figure 4.19** Plots of ln α versus 1/T of six dichloro-substituted PAMEs on GSiAc column

150 °C

$(1/T=2.36\times10^{3} K^{1})$

(a)

$\alpha = 1.019$

(b)

$\alpha = 1.013$

(c)

(d

(e)

$\alpha = 1.061$

(f)

| 6 | 7 | 8 | 9 | 10 | 11 | 12 |

time (min)

Figure 4.20 Chromatograms of (a) **2,3Cl** (b) **2,4Cl** (c) **2,5Cl** (d) **2,6Cl** (e) **3,4Cl** and (f) **3,5Cl** at 150 °C on GSiAc column

Results for di-substituted PAMEs obtained from GSiAc column were compared to those previously obtained from BSiAc column [12]. Both columns could separate enantiomers of all six difluoro-substituted PAMEs and showed poor enantioseparation on dimethyl-substituted PAMEs. However, on BSiAc column, the highest $-\Delta\Delta H$ value was observed for **3,4Me**. Only 2,3-disubstituted PAMEs of all types of substitution could be enantioseparated by both columns.
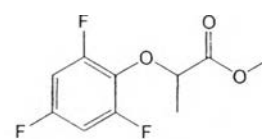
Group 3: PAMEs with substitutions on the aromatic ring
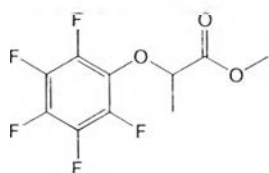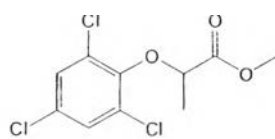
| pentaF | 2,4,6Cl | 2,4,6F |

Enantiomers of PAMEs in Group 3 were methyl 2-phenoxypropanoate derivatives with tri-substitution and penta-substitution on the aromatic ring as shown above. Types of substituent were fluoro and chloro. Disappointingly, other tri-, tetra- and penta-substituted analytes and their isomers were not obtainable. Therefore, a trend on the effect of number of substitution on the aromatic ring could not be clarified.

GSiAc column could separate enantiomers of all three PAMEs in Group 3 as seen from enthalpy difference ($-\Delta\Delta H$) shown in Figure 4.5. However, BSiAc column showed no enantioseparation for 2,4,6Cl [12]. This pointed to the significant of size of cyclodextrin in enantioseparation.

H, an analyte with no substitution on the aromatic ring and pentaF, an analyte with five substitutions on the aromatic ring were considered. H was more retained in GSiAc column than pentaF as seen from plots of ln k'_2 versus 1/T in Figure 4.21. It referred that there was stronger interaction between H and GSiAc phase. Also, H had better enantioselectivity than pentaF for all studied temperature with sharper slope of ln α versus 1/T plot (Figure 4.22) and higher $-\Delta\Delta H$ value. It could be implied that enantioseparation of H could be easily improved with a slight decrease in temperature, compared to pentaF. The separation of H and pentaF at 140 °C and 130 °C were shown in Figure 4.23.

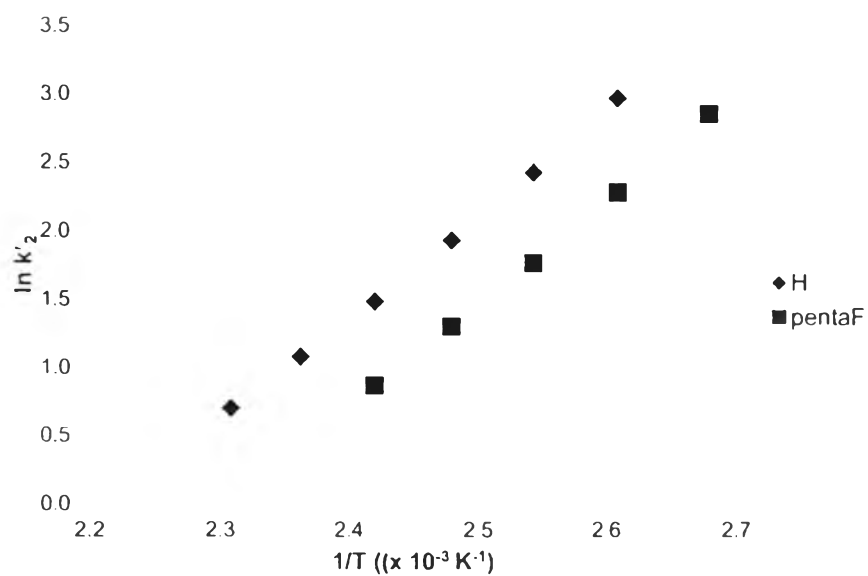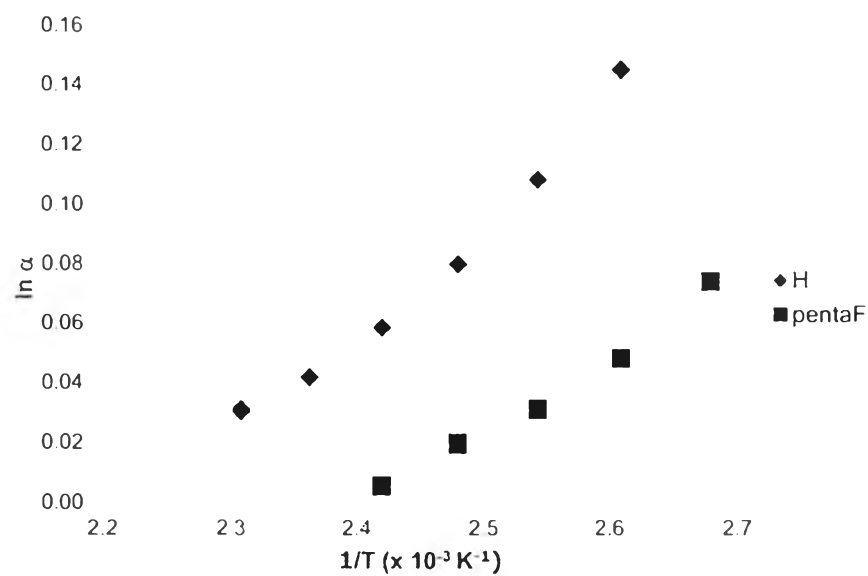Figure 4.21 Plots of ln k′$_2$ versus 1/T of H and pentaF on GSiAc column

Figure 4.22 Plots of ln α versus 1/T of H and pentaF on GSiAc column

140 °C

130 °C

$(1/T = 2.42 \times 10^3 \ K^{-1})$

$(1/T = 2.48 \times 10^3 \ K^{-1})$

(a) H

$\alpha = 1.060$

$\alpha = 1.083$

(b) pentaF
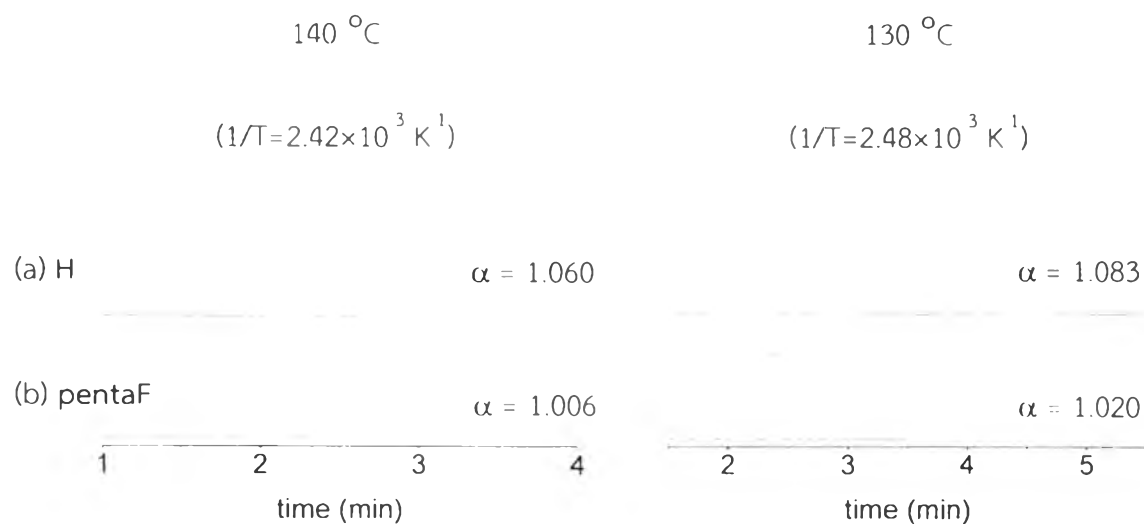
$\alpha = 1.006$

$\alpha = 1.020$

Figure 4.23 Chromatograms of H and **pentaF** at 140 °C (left) and 130 °C (right) on GSiAc colum